Structural influence of alumina in Zn-Cd-Pb phosphate glasses

Jean-Jacques Videau, Abdelouahab El Hadrami, Christine Labrugère, Michel Couzi, Lionel Montagne, Mohamed Mesnaoui, Mohamed Maazaz

Structural influence of alumina in Zn-Cd-Pb phosphate glasses

J.-J. Videau,*[a] A. El Hadrami,[a,d] C. Labrugère,[a] M. Couzi,[b] L. Montagne,[c] M. Mesnaoui,[d] and M. Maazaz [d]

a Institut de Chimie de la Matière Condensée de Bordeaux, UPR 9048, Université de Bordeaux 1, 87 Avenue Dr Albert Schweitzer, 33608 Pessac cedex, France

b Laboratoire de Physico-Chimie Moléculaire UMR 5803, Université de Bordeaux 1, 351, cours de la Libération, 33405 Talence cedex, France

c Unité de Catalyse et de chimie du solide, UMR CNRS 8181, Université des Sciences et Technologies de Lille, Ecole Nationale Supérieure de Chimie de Lille, 59655 Villeneuve d'Ascq cedex, France.

d Laboratoire de Chimie du Solide Minéral, Faculté des Sciences Semlalia, B.P 2390 Marrakech, Marocco

A structural investigation of $(100-y)[50P_2O_5–15ZnO–(35-x)PbO–xCdO]–yAl_2O_3$ polyphosphate glasses was carried out using Raman, NMR (^{31}P, ^{207}Pb and ^{27}Al) and XPS spectroscopies. In alumina-free glasses (y=0), the CdO substitution for PbO induces a strengthening of the network formation, up to x=20. For x>20, the network connectivity decreases because less cations are located in network former sites. In aluminophosphate glasses (x=20 and $0<y\leq8$) the determination of oxygen sites distribution, evaluated from the ^{31}P NMR data, agrees with the O1s XPS results and reveals the formation of Al–O–Al bonds. The compositional dependence of glass structure and properties is qualitatively understood using structural investigations and site distribution. The partial dissolution of alumina in the glass results from the strong network connectivity of the basic compositional glass (x=20). For the $0\leq y<4$ compositional range, the Al^{3+} cations are mainly incorporated in six-fold coordination, and have a limited effect on the glass network. On the contrary for $x\geq4$, a conjugated effect of the multiplicity of the Al coordination number (4, 5 and 6) together with the Al–O–Al bridges contributes increasingly to the compactness and the connectivity of the polyphosphate network. This leads to a large improvement of properties, such as a higher resistance to water corrosion (6×10^{-10} g cm^{-2} min^{-1} at 22°C).

1. Introduction

In our previous reports,[1,2] zinc lead cadmium phosphate glasses have been proposed as efficient storage matrices for heavy and toxic metals such as Pb and Cd. Their compositional dependence of density, glass transition temperature, Vickers microhardness and chemical durability were described. The partial substitution of CdO for PbO in $50P_2O_5–15ZnO–(35-x)PbO–xCdO$ glasses has shown a significant effect on their chemical durability. The chemical durability of phosphate glasses can be also improved by nitrogen or trivalent cations (Al^{3+}, Fe^{3+}) addition in order to reticulate the phosphate network (see for instance Refs 3–5). In our case, Al_2O_3 was chosen to stabilise the host matrix containing the toxic metals (Pb, Cd).[1] A large improvement of the durability was observed, leading to a dissolution rate of 10^{-10} g cm^{-2} min^{-1} at room temperature.[2]

The structural role of ZnO or PbO in binary phosphate glasses has been studied using various techniques such as Raman scattering,[6,7–11] IR spectroscopy,[7,12–13] x-ray photoelectron spectroscopy (XPS),[14–17] x-ray scattering,[18–21] molecular dynamics simulation[22] and nuclear magnetic resonance (NMR).[6,23,24] The structural role of Zn^{2+} or Pb^{2+} cations in the phosphate network is complex owing to their relatively high field strength (z/a^2 with z: ion valence and a: ionic radii of cation[25]). It is thus quite different from pure modifying cations like alkali or alkaline earth cations. Indeed, at high contents in phosphate glass compositions, they may participate in the glass network.[6,18,24–26] The simultaneous admixture of PbO and ZnO in phosphate glass compositions adds to the complexity of the glass structure, and the role of each cation depends not only on the content of each other, but also on the P_2O_5 concentration.[27–30]

The role of Al_2O_3 on the structure of phosphate glasses has been extensively studied.[4,31–35] The change of properties upon introduction of Al_2O_3 to $NaPO_3$ glass can be interpreted in terms of structural changes of the network.[4] (i) The first Al_2O_3 addition results in the depolymerisation of $NaPO_3$ metaphosphate chains, but the Al^{3+} cations in six fold coordination increase the glass network connectivity. The balance of these two effects produces an increase of the glass transition temperature and a decrease in the thermal expansion coefficient. (ii) Above 10% Al_2O_3, a levelling off of properties is observed, which results from a

* Corresponding author. Email videau@icmcb-bordeaux.cnrs.fr

transition from a metaphosphate to an aluminophosphate network, due to the formation of tetrahedral Al^{3+} cations and orthophosphate groups, which have less effect on the strength of the glass network.

The development of phosphate glasses for waste disposal will necessarily lead to complex glass formulations. Our aim has been to propose an investigation of phosphate glasses containing up to five oxides. This paper reports the local structure and group connectivity of the $50P_2O_5$–15ZnO–(35–x)PbO–xCdO and (100–y)($50P_2O_5$–15ZnO–15PbO–20CdO)–$y Al_2O_3$ glasses. The first series describes the effect of lead and cadmium substitution on the structure a zinc metaphosphate glass composition. This structural approach will enable one to understand the compositional dependence of glass structure on the properties that were reported previously.[1] More particularly, the large composition dependence of the chemical durability will be discussed.[2] The effect of alumina addition on the structure and properties of these complex glasses will then be described. Complementary spectroscopic methods were used: Raman scattering, XPS (at the O1s level), and ^{31}P, ^{207}Pb and ^{27}Al solid state NMR.

2. Experimental procedure

The (100–y)[$50P_2O_5$–15ZnO–(35–x)PbO–xCdO] –$y Al_2O_3$ glasses will be labelled subsequently in the text as ZnPbCdP (y=0) and ZnPbCdPAl (x=20 and y>0), They were prepared as previously described.[1]

2.1. Raman spectroscopy

The Raman spectra were recorded with a Labram confocal micro-Raman instrument from Jobin–Yvon (typical resolution of 4 cm^{-1}), in backscattering geometry at room temperature. The system consists of a holographic notch filter for Rayleigh rejection, a microscope equipped with 10×, 50× and 100× objectives (the latter allowing a spatial resolution of less than 2 μm), and CCD detector. The source used for excitation was a He–Ne laser, with an output power of about 10 mW at 632·8 nm. The glass samples have been cut into parallelepipeds about 1×1×1 cm^3, with one surface carefully polished.

2. 2. Nuclear magnetic resonance (NMR)

The solid state ^{31}P NMR experiments were performed on a Bruker ASX 100 spectrometer operating at a Larmor frequency of 40·53 MHz. The ^{31}P MAS NMR spectra were recorded at 5 kHz spinning rate using pulse duration of 3 μs (π/6) with recycle delay time of 60 s to ensure no saturation. The spectra were referenced to an 85% H_3PO_4 solution and decomposed into Gaussian components, using the DMFIT program,[36] assuming that the chemical shift distribution governs ^{31}P NMR line shape of phosphate glasses.

^{207}Pb NMR spectra were recorded on a Bruker ASX400 spectrometer at a Larmor frequency of 83·7 MHz (9·4 T). The ^{207}Pb NMR spectra of glass samples are dominated by large chemical shift anisotropy, due to the large electronic shielding on lead nuclei. The spectra are so wide that MAS does not yield any resolution enhancement, they are thus acquired as static echoes. The pulse length was 1·5 μs and 3 μs, with 15 ms delay time, and the recycling delay was 5 s. ^{207}Pb chemical shifts are referenced relative to a 0·5 M $Pb(NO_3)_2$ solution.

^{27}Al MAS NMR spectra were recorded on a Bruker ASX400 spectrometer at a Larmor frequency of 104·3 MHz, with 15 kHz spinning rate, with a pulse length of 1·5 μs and a recycling delay of 2 s. ^{27}Al chemical shifts are referenced to a 1 M $AlCl_3$ solution.

^{113}Cd NMR spectra could not be recorded on the glasses due to the low sensitivity and concentration of the nucleus.

2. 3. X-ray photoelectron spectroscopy (XPS)

XPS data were collected using a VG Scientific 220i-XL Escalab. Mg K_α x-ray line from the non-monochromatised source (1253·6 eV) was used to acquire O1s areas at constant pass energy of 20 eV. O1s spectra were studied, taking care to estimate the interference from C–O and C–C bonds. Binding energies were referenced to the C1s energy at 284·6 eV. Experimental peaks were fitted using Gaussian–Lorentzian mixture peak fitting software provided by VG Scientific. The half-width of the O1s fitting components was fixed in the 1·6–1·8 eV range. Freshly analysed surfaces were generated by cleaving glasses and immediately introducing them under vacuum.

3. Results and interpretation

3. 1. Raman spectroscopy

Raman spectra of ZnPbCdP samples obtained in the frequency range between 200 and 1500 cm^{-1} are reported in Figure 1. The spectrum of lead zinc metaphosphate (x=0) is similar to the known Raman spectra from other metal metaphosphate glasses.[37] The two main peaks observed at about 700 cm^{-1} and 1160 cm^{-1} have been attributed to the symmetric stretching mode of P–O–P (ν_s POP) bridging bonds and to the symmetric stretching PO_2^- bonds (ν_s PO_2) of PO_4 tetrahedra, respectively.[29] The four shoulders centred at 1160 cm^{-1} (900, 1070, 1240 and 1300 cm^{-1}) have been assigned to the asymmetric stretching mode of P–O–P bridging bonds (ν_sPOP) overlapping the symmetric stretching $(PO_3)^{2-}$ chain end groups ($\nu_s PO_3$), to the asymmetric stretching $(PO_3)^{2-}$ chain end groups ($\nu_{as} PO_3$), to the asymmetric stretching

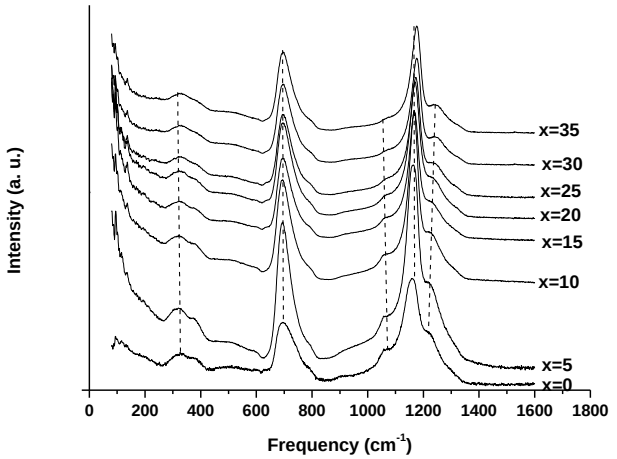

Figure 1. Raman spectra of ZnPbCdP glasses

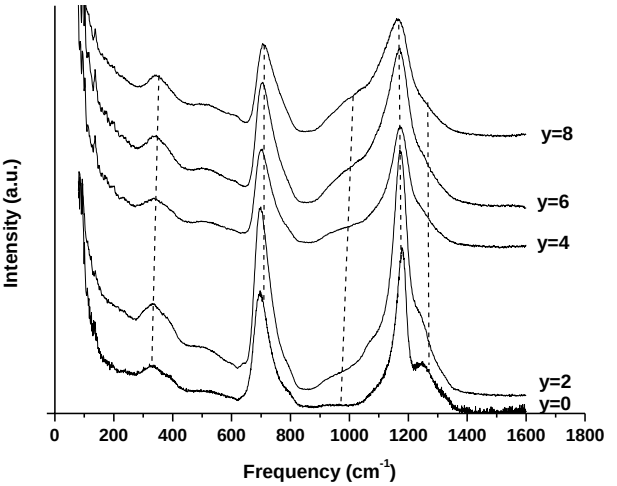

Figure 2. Raman spectra of ZnPbCdPAl glasses

of PO_2^- bonds ($\nu_{as}PO_2$) and to P=O bonds (ν_sP=O), respectively.[27] A weak shoulder close to 800 cm^{-1} could be due to the second symmetric stretching mode of P–O–P bridging bonds (νPOP) in short phosphate units.[38] The weak bands in the 450–600 cm^{-1} range could be assigned to a bending mode related to zinc phosphate network according to Brow *et al*.[6] The low frequency bands, between 300 and 400 cm^{-1}, are related to bending motions of phosphate polyhedral,[6] but the PbO_4 vibration presence is not ruled out in accordance with the study of lead zinc metaphosphate glasses.[29]

The substitution of CdO for PbO in ZnPbCdP glasses (x>0) is not expected to introduce major changes in the glass network (Figure 1). However one can notice (i) a significant shift in νPO_2 (symmetric and asymmetric) with the substitution of CdO for PbO: the $\nu_s PO_2$ and $\nu_{as}PO_2$ bands respectively shift from 1160 and 1220 cm^{-1} for x=0 to 1185 and 1250 cm^{-1} for x=35, (ii) a significant decrease of the relative intensity of $\nu_{as}PO_2$ band compared to the $\nu_s PO_2$ band, as indicated by the $\nu_{as}PO_2/\nu_s PO_2$ intensity ratio values that decreases from 0·5 for x=0 to 0·27 for x=35, (iii) a reduction in intensity of ν_s PO_3 shoulder and of the broad band at 1020 cm^{-1}.

The variations of symmetric and asymmetric stretching modes of PO_2 units can be attributed to the larger field strength of Cd^{2+} (2·22 $Å^{-2}$) compared to Pb^{2+} (1·51 $Å^{-2}$), that affects the metal to nonbridging oxygen bond along phosphate chains. This interpretation agrees with the suggested model of Rouse *et al*[37] in alkali metaphosphate glasses. The model predicts that the frequency of symmetric and asymmetric PO_2 stretch will increase with increasing force constant in the alkali–nonbridging oxygen bond. The effect of substituting Cd^{2+} ions for Pb^{2+} ions in metaphosphate glass is an increase in the force constant as a result of its higher field strength. The progressive change in relative band intensities ($\nu_{as}PO_2$, $\nu_s PO_2$) with the Cd^{2+} substitution indicates a decrease of the asymmetry of the electronic distribution on the nonbridging oxygen atoms, due to the Pb^{2+} electronic lone pair. The simultaneous decrease in intensity of the bands of PO_3^{2-} end-groups and PbO_4 units as Pb^{2+} content decreases can be interpreted as a reticulation of phosphate chains by Cd^{2+} ions.

The Raman spectra for ZnPbCdPAl glasses are reported in Figure 2. The Al_2O_3 addition induces a broadening of the two main bands (ν_s POP and ν_s PO_2, around 700 and 1200 cm^{-1}, respectively), and a significant growth of a shoulder at ~1000 cm^{-1}, particularly for y≥4. Moreover, when y increases, the frequency of the ν_s PO_2 band maximum decreases from 1172 to 1164 cm^{-1} and a reverse behaviour affects the ν_s POP band (from 697 to 710 cm^{-1}). The alumina addition progressively induces a weak shift of the ν_s PO_2 band and the appearance of a shoulder (around 1000 cm^{-1}), indicating a moderate depolymerisation of the phosphate network. The increase of ν_s POP band frequency with y can be assigned to POP bond strengthening induced not only by a shortening of phosphates chains but also by a weakening of the antagonistic PO^- bond due to an increase of the bond covalence between Al^{3+} cations and nonbridging oxygen atoms. The additional asymmetry of the high frequency side of ν_s POP band can be assigned to the presence of Al^{3+} ions in coordination lower than 6 (see below ^{27}Al NMR results).[32]

3. 2. ^{31}P MAS NMR spectroscopy

Figure 3(a) shows the ^{31}P MAS NMR spectra for ZnPbCdP glasses. These spectra can be decomposed into three components with the same shape for all x values. An example of decomposition is shown for the x=20 sample in Figure 3(b). When x increases, the low field component shifts from −10 to −7 ppm, and the main component varies from −26 to −28 ppm. The third resonance at −41 ppm remains at the same frequency when x varies. These resonances can

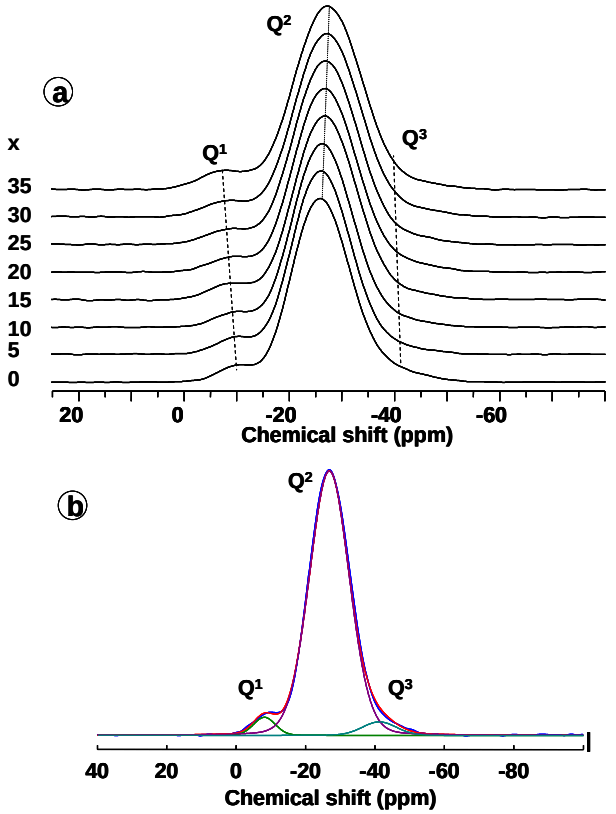

Figure 3. (a) ^{31}P MAS NMR spectra of ZnPbCdP glasses. (b) Example of decomposition of ^{31}P MAS NMR spectra for the x*=20 glass*

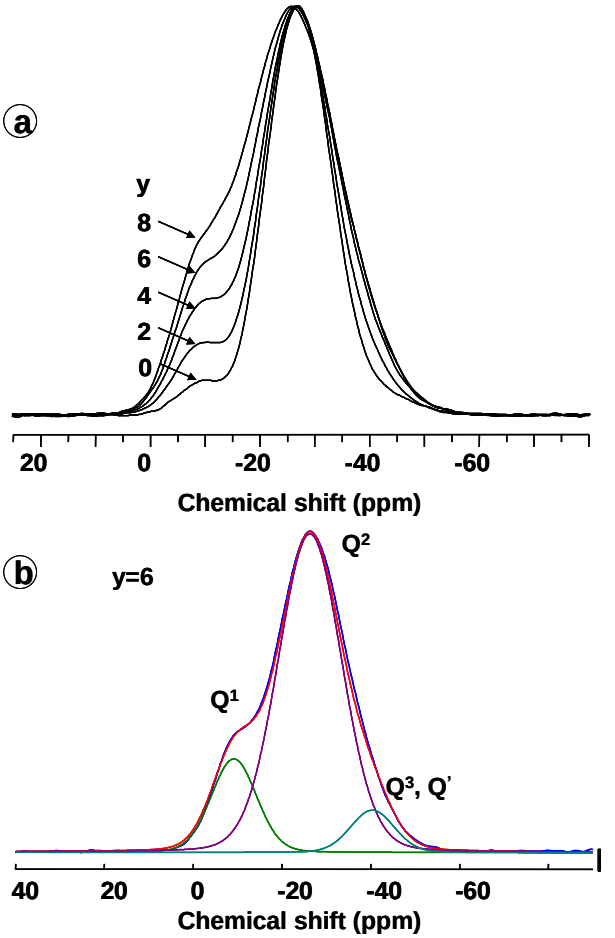

Figure 4. (a) Normalised ^{31}P MAS NMR spectra of ZnPbCdPAl glasses. (b) Example of decomposition and assignment of the ^{31}P MAS NMR spectrum of the y*=6 glass*

be assigned respectively to Q^1, Q^2 and Q^3 sites, in agreement with the attribution of the isotopic chemical shifts for Zn,[6,23] Pb[26] and Cd[39] polyphosphate glasses reported in Table 1. It is worth noting that no Q^3 site was reported in zinc lead metaphosphate glasses.[23] The resonance around −10 ppm has been interpreted by Liu *et al*[29] as Q^2 bonded to one lead atom. In our case, the assignment of the deshielded component to Q^1 site agrees with the presence of Q^3 sites owing to the disproportionation reaction $2Q^2 \leftrightarrow Q^1 + Q^3$.[40] If the activity coefficients for each Q^i sites are equal and if this reaction is treated as a true chemical reaction, an equilibrium constant (k_2) can be estimated following the equation: $k_2=[Q^1][Q^3]/[Q^2]^2$. Using the estimated site concentration determined from the component areas ($[Q^2]=0{\cdot}92\pm10^{-3}$, $[Q^1]=[Q^3]=0{\cdot}04\pm10^{-3}$), k_2 is $2\times10^{-3}\pm10^{-4}$. This value is slightly higher than that obtained for lead metaphosphate.[26] Since no disproportionation of Q^2 sites appears in zinc[6,23] and cadmium[39] metaphosphate glasses, the presence of Q^1 and Q^3 sites in our glasses could be induced by the simultaneous presence of the three divalent cations.

*Table 1. ^{31}P MAS NMR isotropic chemical shifts of ZnPbCdP glasses and zinc, lead and cadmium polyphosphate glasses; *indicates the isotropic chemical shifts of metaphosphate compositions*

	Chemical shift (ppm)			
Sites	*$ZnO–P_2O_5$*[6,23]	*$PbO–P_2O_5$*[26]	*$CdO–P_2O_5–Al_2O_3$*[39]	*This work*
Q^1	−13 to −16 (−13)*	−8 to −10 (−9·7)*	−6·5 to −10·8 (−6·7 to −7·5)*	−7 to −10
Q^2	−26 to −33 (−31*)	−20 to −25 (−24·6*)	−23 to −32 (−27)*	−26 to −28
Q^3	−38 to −46	(−38·3)*	−41 to −46	−41

The observed changes in ^{31}P isotropic chemical shifts (δ_{iso}) with x values are related to the nature of the next-nearest-neighbour bonding of P nuclei via the oxygen atoms, i.e. the modifying cations. The substitution of CdO for PbO induces a shielding of the P nucleus in Q^2 sites (δ_{iso} becomes more negative) and a deshielding of the P nucleus in Q^1 sites (δ_{iso} becomes less negative). According to Brow *et al*,[24] the Q^2 shielding can be calculated from the linear correlation: $\delta_{iso}(\text{ppm})=-14{\cdot}6-6{\cdot}0(z/r)$. This relation can be extended to mixed metaphosphate glasses and becomes: $\delta_{iso}(\text{ppm})=-14{\cdot}6-6{\cdot}0[\sum c_i(z_i/r_i)]$ where c_i is the molar fraction, z_i is the charge and r_i is cationic radii for each component i, i.e. Zn, Cd and Pb (in octahedral coordination). The calculated (δ_{iso}=−26·2 and −28·4ppm) and experimental (δ_{iso}=−26 and −27

Table 2. Isotropic chemical shifts (δ_{iso}) and relative areas of ^{31}P NMR component of ZnPbCdPAl glasses

	Q^1		Q^2		Q^3, Q'	
y	δ_{iso} (ppm)	%	δ_{iso} (ppm)	%	δ_{iso} (ppm)	%
0	−8·1	3·5	−26·8	93·1	−41·3	3·4
2	−8·5	7·8	−26·9	88·9	−41·3	3·6
4	−8·8	10·9	−26·8	83·8	−41·1	5·4
6	−9·2	15·7	−26·3	77·3	−40·2	7
8	−9·7	16·7	−25·8	76·8	−40·1	6·5

ppm) values for x=0 and x=35, respectively, are in good qualitative agreement, which means that Cd^{2+} substitution is homogeneous around the Q^2 sites. The full width at half maximum (FWHM) is also proportional to the ionic potential and increases with z/r.[24] Thus, the FWHM for x=0 glass (13 ppm) is lower than that for x=35 glass (16 ppm) since the z/r value of Pb^{2+} (1·74 $Å^{-1}$) is lower than that of Cd^{2+} (2·11 $Å^{-1}$). These FWHM values are included between those of lead and cadmium metaphosphate glasses (10 and 19 ppm, respectively), thus confirming a homogeneous distribution of cations on Q^2 sites.

The ^{31}P MAS NMR spectra of ZnPbCdPAl glasses are reported in Figure 4(a). As in ZnPbCdP glasses, the spectra of ZnPbCdPAl glasses can be decomposed in three components, which are assigned to Q^1, Q^2 and Q^3 sites. Their chemical shifts and relative areas are reported in Table 2. An example of assignment is given for y=6 glass sample in Figure 4(b). The chemical shifts and the relative area of each component are reported in Table 2. The Q^2 component centred at −26·8 ppm for y=0 decreases in intensity with y and slightly shifts towards less negative values. Generally, a deshielding (shift to more positive values) of the P nucleus of Q^2 sites is expected when the metaphosphate chain length decreases. In contrast, the presence of Al^{3+} cations (high cationic field strength) as next-nearest-neighbour of phosphorus, tends to shift strongly the Q^2 component to high field (shielding effect).[4] The small observed δ_{iso} shift (1 ppm) must thus be considered to result from these two antagonist effects. The component at δ_{iso}=−8·1 ppm (y=0), ascribed to Q^1 sites, increases in intensity and shifts to −9·7 ppm for y=8. This peak is ascribed to Q^1 sites bonded to Al^{3+} cations probably in octahedral coordination, in accordance with other studies.[31,35] The component attributed to Q^3 sites in ZnPbCdP glasses does not exhibit any change for y=0 and 2 and then its chemical shift changes towards less negative values. The assignment to Q^3 sites must be ruled out for y>2 since ^{27}Al MAS NMR shows (see below) that part of Al^{3+} cations is in lower coordination (4 and 5), and thus the shielding of phosphorus should increases owing to the increase of field strength potential of Al(4 and 5) compared to Al(6).This could indicate the presence of a new site, i.e. Al^{3+} cations coordinated to either Q^1 (labelled Q^1_{Al}) or Q^2 (Q^2_{Al}) or both sites (labelled Q′). Such site could have a chemical shift overlaying the Q^3 one according to the range of isotropic chemical shift values reported by Grimmer *et al*[41] for aluminophosphate crystals (35–45 ppm).

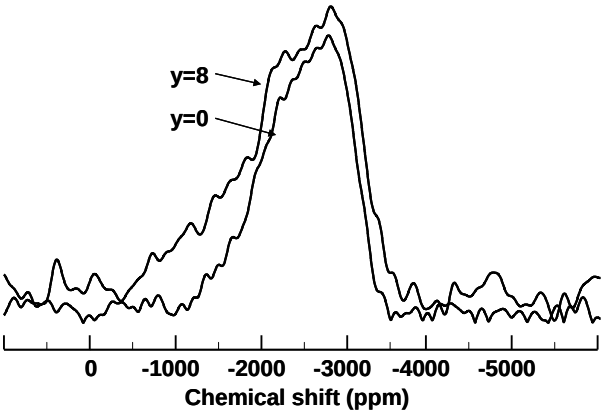

Figure 5. ^{207}Pb NMR spectra of y=0 and 8 ZnPbCdPAl glasses

3. 3. ^{207}Pb MAS NMR

^{207}Pb MAS NMR spectra for two extreme glass compositions (y=0 and y=8) of ZnPbCdPAl glasses are presented in Figure 5. The asymmetric and broad lineshapes (HWHH of 2000 ppm) are consistent with a wide site distribution of lead cations. The Al_2O_3 addition into the metaphosphate matrix results in an increase of the intensity of the low field side of the spectrum in the −500 ppm to −1800 ppm chemical shift range. This variation reveals a modification of the Pb^{2+} cation environment when y increases. The comparison with the chemical shifts of crystalline lead polyphosphate[42] suggests that the alumina addition induces more covalent Pb–O bonds than in ZnPbCdP glasses, which reveals an increase of the network former role of PbO in ZnPbCdPAl glasses.

3. 6. ^{27}Al MAS NMR

Figure 6 reports the ^{27}Al MAS NMR spectra (normalised to the most intense resonance) of ZnPbCdPAl glasses (y=2, 4, 6 and 8). The three resonances centred at 34, 5 and −18 ppm are assigned to $Al(OP)_4$, $Al(OP)_5$ and $Al(OP)_6$ units, respectively. Similar assignments were given for sodium, lead and cadmium aluminophosphate glasses.[4,31,39,43] No detectable change of ^{27}Al chemical shift appears when y increases. The

Table 3. Relative peak areas of $Al(OP)_4$, $Al(OP)_5$ and $Al(OP)_6$ units, and average Al coordination number, deduced from ^{27}Al MAS NMR spectra of ZnPbCdPAl glasses

y	$Al(PO_4)_4$ (%)	$Al(PO_4)_5$ (%)	$Al(PO_4)_6$ (%)	Al CN (%)
2	7	14·5	78·5	5·72
4	17	21	62	5·45
6	27	22	51	5·24
8	39·5	22	38·5	4·63

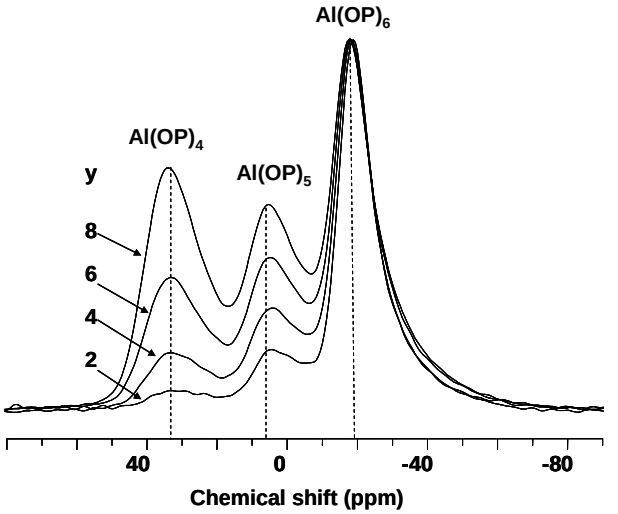

Figure 6. ^{27}Al MAS NMR spectra of ZnPbCdPAl glasses

$Al(OP)_6$ unit contribution dominates the spectra but its intensity progressively decreases (Table 3), which indicate a decrease of the Al coordination when *y* increases. This result differs from the previous ^{27}Al MAS NMR in sodium aluminophosphate glasses, which showed that the $Al(OP)_6$ units dominate up to about 10% of alumina.[31]

3. 7. XPS

The decomposed O1s spectra of *x*=20 ZnPbCdP and *y*=6 ZnPbCdPAl glass samples are shown in Figure 7. The relative areas as function of *y* are reported in Table 4. As reported on sodium phosphate glasses,[16] on zinc phosphates glasses[15] and on more complex glasses such as sodium aluminophosphate[31] or sodium borophosphate,[44] the low (≈531 eV) and the high (≈533 eV) energy components (Table 4) are assigned to the nonbridging oxygen atom (O_{nb}) in the P–O_{nb}–M′ bond (where M′ is a network modifier cation), without differentiating between P–O^- and P=O bonds,[45] and to symmetric bridging oxygen atom (O_b) in the P–O_b–P bridge, respectively. The intermediate component (≈532 eV) can be attributed to other asymmetric bridging oxygen atoms (O′) in the P–O′–M′′ bridges, for which the O′–M′′ bonds are more covalent that O_{nb}–M′ but less covalent than that of O_b–P. M′′ cations are in a low coordination state or/and present a high electrostatic field strength, thus assuming a partial network former role. The relative intensities of the O1s components remain unchanged (Table 4) with the first substitution of CdO for PbO, which is similar to Zn-Pb metaphosphate glasses.[30] These authors[30] calculated that the proportion of PbO entering in the glass network (i.e. with a low coordination number) is included between 5 and 9 mol%, for 30 and 40 mol% PbO in glass, and the remaining part assumes a modifier role similar to Zn^{2+}

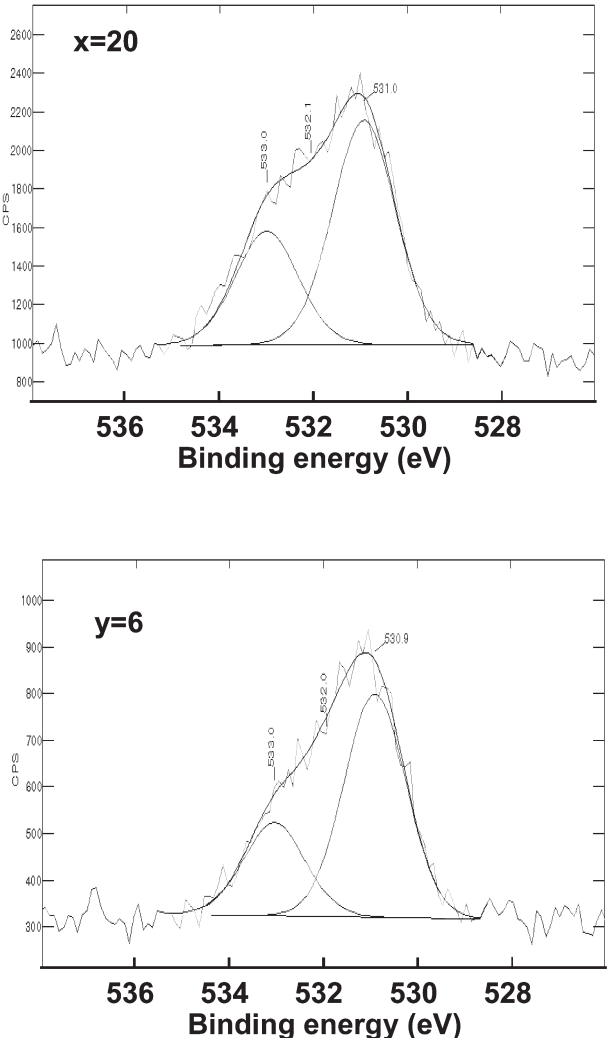

Figure 7. Examples of decomposition of XPS O1s spectra of x*=20 ZnPbCdP glass and* y*=6 ZnPbCdPAl glass*

cations. In our glasses, for *x*>20, the increase of O_{nb} at the expense of O′ can be related to the decrease of the proportion of network former cations (probably Pb^{2+} cation in low coordination).

Three components are necessary to fit the O1s signal of ZnPbCdPAl glasses, as in ZnPbCdP glasses.

Table 4. Relative peak areas of O_b, O′ and O_{nb} components of decomposed O1s XPS spectra of ZnPbCdP (x) *and ZnPbCdPAl* (y) *glasses*

x	*Ob (%)*	*O′ (%)*	*Onb (%)*
0	32	14	54
5	31	16	53
10	31·5	14·5	54
15	32	14	54
20	32	15	53
25	32	14	54
30	32	13	55
35	32	10	58
y			
0	32	15	53
2	30	18	52
4	29	20	51
6	28	22	50
8	27	23	50

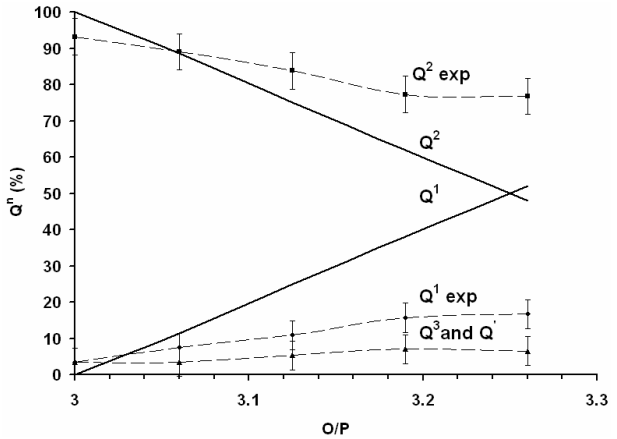

Figure 8. Fractions of Q^n sites deduced from the decomposition of ^{31}P MAS NMR spectrum (dashed line), compared to those calculated (continuous line) assuming a complete dissolution of Al_2O_3 in the ZnPbCdP melt

The increase of the Al_2O_3 content leads to a small decrease of the O_{nb} and O_b areas, compensated by an increase of O′ fraction (Table 4). It is noteworthy that the O′ component here includes not only the P–O′–M′′ bonding but also P–O′–Al. Moreover, Al–O′–Al bridges, which will be discussed in the next section, can be also included in this component.

4. Discussion

4. 1. Phosphate site distribution in ZnPbCdPAl glasses

The presence of Q^1 sites on ^{31}P MAS NMR spectra (Figure 4) indicates that the dissociation of Al_2O_3 in phosphate melt occurs according to the pseudo-reaction

$$2Q^2 + Al_2O_3 \rightarrow 4Q_1$$

The dissociation of oxides (ZnO,[6] CdO,[39] Al_2O_3[4] or Bi_2O_3[45]) in phosphate melts is generally complete. This can be verified by comparing the fraction of Q^n sites, measured by the decomposition of ^{31}P MAS NMR spectra, with the values calculated with the following equations

$$f\left(Q^2\right) = \frac{3\cdot 5 - (O/P)}{0\cdot 5} \times 100$$

$f(Q^1)$=100–f(Q^2) for 3≤O/P≤3·5

$$f\left(Q^1\right) = \frac{4 - (O/P)}{0\cdot 5} \times 100$$

$f(Q^0)$=100–$f(Q^1)$ for 3·5≤O/P≤4

$f(Q^0)$=100 for O/P≥4

Figure 8 reports the variation of the measured Q^n_{exp} fractions, compared to the Q^n site fractions calculated assuming a complete dissolution of Al_2O_3 in the ZnPbCdP melt versus the atomic O/P ratio. Notice that the use of oxygen/phosphorus ratio (O/P) instead of the composition avoids the need to consider the valence of the cations in the calculation of the fraction of Q^n sites. A large discrepancy between calculated and experimental values is observed on Figure 8. Experimental data for Q^2_{exp} sites are overestimated, whereas those for Q^1_{exp} are underestimated. This indicates that the dissociation of Al_2O_3 in ZnPbCdPAl melt is not complete, and that Al–O–Al bonds must remain in the glasses. No Al–O–Al resonance (close to 10 ppm[4]) is observed on ^{27}Al NMR MAS spectra (Figure 6), but they could overlapped by the $Al(OP)_5$ resonance.

4. 2. Oxygen site distribution in ZnPbCdPAl glasses

From the fitting of ^{31}P NMR spectra (including Q^1, Q^2, Q^3 and $Q^{'}$ sites) it is possible to quantify the four expected sites, i.e. P–O–P, P–O–M (M=Zn, Cd and Pb), P–O–Al and Al–O–Al. The calculation is conducted with the following steps:

(i) calculation of phosphorus atom number (m_P=1−x) from the glass composition and the phosphorus atom number in Q^n sites: $m_{Q^n} = f(Q^n)m_P$ where $f(Q^n)$ is the Q^n site fraction. We assume that $f(Q^3)$ remains constant with y, in accordance with the unchanged value (3·4%) between y=0 and y=2,

(ii) calculation of the quantity of bridging oxygens P–O–P (m_{P-O-P}) and nonbridging oxygens P=O and P–O^-(M,Al) ($m_{P=O}$ and $m_{P-O^-(M,Al)}$) for a given Q^n site, knowing that Q^2 site gives 1×P=O, 1×P–O^-(M,Al) and 1×P–O–P, Q^1 site gives 1×P=O, 2×P–O^-(M, Al) and 1/2×P–O–P and Q^3 site gives 1×P=O, 3/2×P–O–P.

The oxygen atom quantities are

$m_{P=O} = m_{Q^3} + m_{Q^2} + m_{Q'} + m_{Q^1}$ ($m_{Q'}$:$m_{Q^1{}_{Al}}$ and/or $m_{Q^2{}_{Al}}$)

$m_{P-O^-(M,Al)} = m_{Q^2} + m_{Q'} + 2m_{Q^1}$ ($m_{Q'}$:$2m_{Q^1{}_{Al}}$ and/or $m_{Q^2{}_{Al}}$)

$m_{P-O-P} = 3/2m_{Q^3} + m_{Q^2} + m_{Q'} + 1/2m_{Q^1}$ ($m_{Q'}$:$1/2m_{Q^1{}_{Al}}$ and/or $m_{Q^2{}_{Al}}$)

and the sum is $m_O = m_{P=O} + m_{P-O^-(M,Al)} + m_{P-O-P}$

(iii) calculation of the oxygen atom quantity in Al–O–Al bonds ($m_{Al-O-Al}$) corresponding to the difference of oxygen atom quantity calculated from the glass composition ($m_{O\ comp}$) and m_O,

(iv) calculation of nonbridging oxygen atoms (m_{P-O^-M}, and m_{P-O^-Al}) with the assumption that all M ions are linked to phosphorus atoms, which is justified by the larger oxoacidity of P_2O_5 than Al_2O_3. Accordingly, the oxygen atom quantity in P–O^-M bonds (m_{P-O^-M}) corresponds to the quantity of M atom number derived from the composition ($m_{M\ comp}$). The remaining quantity of oxygen atom in P–O^-(M,Al) bonds can be associated to the P–O–Al bonds ($m_{P-O-Al} = m_{P-O^-(M,Al)} - m_{P-O^-M}$). Moreover, the P=O bonds can be linked to M atoms, which is expressed as: $m_{P=O}/m_{P-O^-(M,Al)}$. Consequently, the final formulation of the oxygen atom number in P–O^-–M (m'_{P-O^-M}) and in P–O–Al

Table 5. Fraction of oxygen species in ZnPbCdPAl glasses, calculated from the ^{31}P NMR MAS spectra

x	*P–O–P (%)*	*P–O–M (%)*	*P–O–Al (%)*	*Al–O–Al (%)*
0	33·3	66·7	0	0
2	32	64	2·6	1·4
4	30·3	61·4	4·7	3·6
6	28·9	58·6	7·3	5·2
8	28·2	58	7·7	6·1

bonds (m'_{P-O-Al}) are $[m_{P=O}][1+(m_{P=O}/m_{P-O^-_{-(M,Al)}})]$ and $[m_{P-O^-_{-(M,Al)}}\text{-}m_{P=O}][(1+m_{P=O}/m_{P-O^-(M,Al)})]$, respectively. The sum of m_{P-O-P}, m'_{P-O^-M}, m'_{P-O-Al} and $m_{Al-O-Al}$ corresponds to $m_{O\ comp}$. The quantification of the different oxygen atom sites is reported in Table 5. It confirms the existence of Al–O–Al bridges, but they always remain in minor quantity compared to P–O–Al bridges. This result thus confirms that the dissolution of Al_2O_3 is not complete in the ZnPbCdPAl phosphate network. The quantification of the oxygen sites carried out from the NMR or the XPS does not systematically lead to the same relative quantity of oxygen species, excepted for POP (table 5) and P–O_b–P (Table 4). A difference between P–O_{nb}–M′ (Table 4) and P–O–M (Table 5) occurs owing to the fact that the first relates primarily to the cations playing the role of network modifier (M′) whereas the second includes all the cations (M′ and M′′). Moreover, the O′ species derived from XPS (Table 4) correspond to (Al, P)–O′–(M′′,Al) bridges, but not to (Al,P)–O–Al bridges derived from NMR, which gather P–O–Al and Al–O–Al bridges (Table 5). The subtraction of the fractions of (Al,P)–O–Al bridges with (Al,P)–O′–(M′′,Al) bridges (Table 4) makes it possible to reach the P–O–M′′ (labelled P–O–M′′ (cal.)) fraction values and by addition of the latter with P–O_{nb}–M′ we calculate P–O–M (labelled P–O–M (cal.)). This enables the comparison with the P–O–M fraction obtained starting from the ^{31}P NMR spectra (Table 5).

Figure 9 reports the variation in the oxygen fractions obtained from (i) experimental O1s XPS spectra, (ii) ^{31}P NMR spectra data with Q^1_{Al} sites ranked as Q′ sites for calculation (Q^2_{Al} sites giving approximate result) and (iii) calculations as described above. The similarities of the fractions of P–O–M (NMR) and P–O–M (cal.) on the one hand, and of P–O–P (NMR) compared to P–O_b–P (XPS), validate the method of quantification of the oxygen species from the ^{31}P NMR spectra. The P–O–M′′ (cal.) value progressively decreases in the *y* compositional range. This indicates that the M''^{2+} ions located in position of network former are in competition with the lower coordinated Al^{3+} ions (Al(4) and (5)). For the low values of *y*, the content of Al^{3+}(4, 5) is too small (Table 3) to be able to replace the M''^{2+} ions. In the intermediate domain of composition, substitution can be done but it appears limited, probably because of their participation in the formation of Al–O–Al bridges (Table 5). For the high value of *y*, the compositions are close to the limit of the vitreous domain. The network seems to be close to saturation in Al_2O_3 and in this case, the AlO_4 tetrahedra would experience even more difficulty of being integrated, in agreement with the deceleration of the rupture of polyphosphate chains (see P–O–P curves in Figure 9) and they thus participate in the increase of Al–O–Al bridge content.

4. 3. Relation between phosphate chain length and Al_2O_3 dissolution in phosphate network

The depolymerisation of the metaphosphate network, expressed as the average chain length *p* (*p*: average

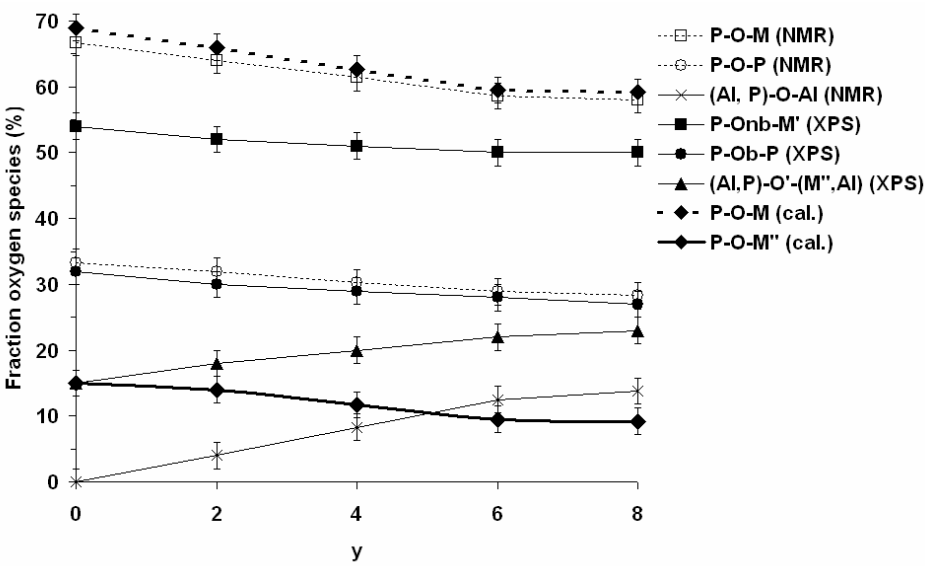

Figure 9. Fractions of oxygen species deduced from the decomposition of 31P MAS NMR spectrum, compared to those obtained from the decomposition of O1s XPS spectra, and calculated as described in the text. The (Al,P)–O–Al (NMR) fraction is the sum of m′P–O–Al and mAl–O–Al fractions (see text and Table 5) and (Al,P)–O′–(M′′,Al) (XPS) fraction is equivalent to O′ (see text and Table 4)

Table 6. Comparison of the average chain length p *and O/P ratio values, assuming a complete and partial (*) dissolution of Al_2O_3 with Al–O–Al bridge formation in ZnPbCdPAl glasses*

y	*p*	*p**	*O/P*	*O/P**
2	24	17	3·04	3·06
4	16	8	3·06	3·13
6	11	5	3·09	3·19
8	10	4	3·10	3·26

number of P atoms into the chain) depends on the Al_2O_3 content participating to the network formation. In case of partial dissolution of Al_2O_3, Al–O–Al bridges are formed, *p* is underestimated and O/P ratio is overestimated. From the ^{31}P NMR quantification of Q^n sites (Table 2), the actual *p* and O/P ratio values can be estimated. In the polyphosphate chains, the average chain length *p* can be expressed to the following relation

$$p=2([Q^1]+[Q^2,Q'])/[Q^1]$$

where $[Q^n]$ are the Q^1, Q^2 and Q' fractions; $[Q']$ is the difference between $[Q^3,Q']$ and $[Q^3]$=3·4% for y=0, with

$$[Q']=50\%[Q^1_{Al}]+50\%[Q^2_{Al}]$$

The O/P values are deduced from the formulation of polyphosphates $[P_pO_{3p+1}]^{(p+2)-}$ as follows

$$O/P=(1/p)+3$$

The values of *p* and O/P are reported in Table 6, they are compared with those (*p**) calculated assuming a total dissociation of Al_2O_3 in the ZnPbCd metaphosphate glass. The results show that the presence of Al–O–Al bridges reduces the apparent depolymerisation degree of the metaphosphate network. This tendency is accentuated when *y* increases, giving relatively long chains (*p* close to 10) at the limit of the vitreous domain.

4. 4. Structure–property relationships

In this section, the descriptions of the ZnPbCdP and ZnPbCdPAl glass structures are used to discuss the relationships between their compositions and properties, previously described in Refs 1 and 2, respectively. The properties investigated were the glass transition (T_g) and crystallisation (T_c) temperatures, the dissolution rate ($V_{dissol.}$) and molar volume (V_M).

The structural investigations of the Cd-free Zn, Pb metaphosphate glass (x=0) reveal that the Zn/Pb substitution produces a depolymerisation effect on the chains with the creation of chain end groups Q^1. This is compensated by a strengthening of the phosphates network by the neutral Q^3 entities. The substitution of Pb^{2+} for Cd^{2+} cations with decreasing ionic radius produces an increase of T_g, water resistance and microhardness up to x=20.[1] This behaviour can be correlated to the strengthening of the bonds between chains and nonbridging oxygen atoms of the phosphate chains by Cd^{2+} cations. The substitution of Cd^{2+} for Pb^{2+} cations in network modifier sites thus induces a network strengthening effect, which is reflected on the evolution of properties. For x>20, $V_{dissol.}$ Increases,[1] which can be interpreted as the result of an excess of Cd^{2+} cations, which enter into modifier sites at the expense of former sites previously (for x<20) occupied by Pb^{2+} cations. This assumption is in agreement with the XPS results (Table 4) and with the dissolution study of these glasses in which the Cd^{2+} cation content leached out from x=35 glass sample is more than twenty time larger than those leached out from x=20 glass sample.[2]

For ZnPbCdPAl glasses, two domains of the relationship between composition and properties could be distinguished. For y≤4, the monotonic increase of T_g and T_c together with microhardness[1] can be related to the excess of $Al(OP)_6$ groups that crosslink the polyphosphate chains, thus leading to a limited improvement in the chemical durability ($V_{dissol.}$). For x>4, the small increase of T_g and microhardness[1] and the abrupt decrease of V_M and $V_{dissol.}$ reflects an increase of compactness and of the strengthening of the glass network. Whereas in the alkali aluminophosphate glasses this effect was attributed to the formation of $Al(OP)_4$ units,[4] it could be here due to the presence of Al–O–Al bridges with a large covalent character, which contributes by crosslinking neighbouring phosphate chains and so counter balances the decrease of Al-coordination number. The network forming effect of Pb^{2+} cation in covalently bonded configurations (see ^{207}Pb NMR section) also contributes to increase the water resistance. This assumption agrees with the corrosion tests showing that only Cd^{2+} and Zn^{2+} cations are leached out at 50°C. The strengthened network of ZnPbCdAl glasses indeed leads to a high resistance to water corrosion.[2] For example, the y=8 glass composition has a dissolution rate close to 6×10^{-10} g cm^{-2} min^{-1},[2] despite its relatively low T_g (450°C).[1] It thus makes it a potential candidate for the immobilisation of toxic heavy metals.

5. Conclusions

Local structure and oxygen bonding of zinc lead cadmium metaphosphate glasses (ZnPbCdP) and aluminium zinc lead cadmium polyphosphate glasses (ZnPbCdPAl) were studied by Raman, NMR ad XPS and were compared with property evolution. The main conclusions are:

1. In ZnPbCdP glasses with metaphosphate stoichiometry, the admixture of cations (Zn, Pb and Cd) generates a partial depolymerisation of phosphate chains (Q^2) with the creation of chain end Q^1 and Q^3 groups. The substitution of Pb^{2+} for Cd^{2+} cations

results in (i) the crosslinking strengthening of phosphate chains by network modifier cations (Cd^{2+} and a majority of Pb^{2+}), and by mixed network former P–O–Pb linkages. This crosslinking effect improves the properties up to x=20, (ii) for x>20, a decrease of the network connectivity is observed, due to the decrease of the quantity of Pb^{2+} cations in network former positions.

2. Alumina addition in the ZnPbCd metaphosphate glass results in an incomplete dissolution of Al^{3+} ions with Al–O–Al bridge formation, attributed to the over strong network character of the basic glass (x=20). The two domains of relationships between composition and properties can be globally distinguished as follows: (i) Al^{3+} introduction in six-fold coordination have a limited effect on ZnPbCd glass network, since it is already strengthened by M^{2+} cations. Consequently, Al(6) has also a limited effect on the properties up to y=4, (ii) the conjugated effects of the decrease of Al-coordination (from 6 to 4, 5) and chain depolymerisation with the presence of Al–O–Al bridges contribute to an increase of compactness and a strengthening of the glass network, leading to a large improvement of properties such as a high resistance to water corrosion for y>4.

Acknowledgements

The authors are thankful to CMIFM (Action Intégrée 187/SM/99) for financial assistance. L. Montagne acknowledges the FEDER, Région Nord Pas-de-Calais, Ministère de l'Education Nationale de l'Enseignement Supérieur et de la Recherche, CNRS, USTL and ENSC-Lille for fundus of NMR spectrometers.

References

1. El Hadrami, A., Aouad, H., Mesnaoui, M., Maazaz, M. & Videau, J.-J. *Mater. Lett.*, 2002, **57**, 894.
2. El Hadrami, A., Mesnaoui, M., Maazaz, M. & Videau, J.-J. *J. Non-Cryst. Solids*, 2003, **331**, 228.
3. Bunker, B. C., Arnold, G. W. & Wilder, J. A. *J. Non- Cryst. Solids*, 1984, **64**, 291.
4. Brow, R. K., Kirkpatick, R. J. & Turner, G. L. *J. Am. Ceram. Soc.*, 1993, **76** (4), 919.
5. Marasmghe, G. K., Karabulut, M., Ray, C. S., Day, D. E., Shuh, W.
   D. E., Allen, P. G., Saboungi, M. L., Grimsdith, M. & Haeffmer, D. *J. Non- Cryst. Solids*, 2000, **263–264**, 146.
6. Brow, R. K., Tallant, D. R., Myers, S. T. & Phifer, C. C. *J. Non-Cryst. Solids*, 1995, **191**, 45.
7. Meyer, K. *J. Non- Cryst. Solids*, 1997, **209**, 227.
8. Bobovich, Y. S. *Opt. Spect.*, 1962, **13** (4), 274.
9. Ray, N. H. Glass Technol., 1975, **16** (5), 107.
10. Nelson, B. N. & Exarhos, G. J. *J. Chem. Phys.*, 1979, **71** (7), 2739.
11. Saoût, G., Le Simon, P., Fayon, F., Blin, A. & Vaills, Y. *J. Raman Spectrosc.*, 2002, **33**, 740.
12. Selvaraj, U. & Rao, K. J. *J. Non- Cryst. Solids*, 1988, **104**, 300.
13. Dayanand, C., Bhikshamaiah, G., Jaya Tyagaraju, V., Salagram, M. & Krisma Murthy, A. S. R. *J. Mater. Sci.*, 1996, **31**, 1945.
14. Brow R. K. *J. Non- Cryst. Solids*, 1996, **194**, 267.
15. Onyiriuka E. C. *J. Non- Cryst. Solids*, 1993, **163**, 268.
16. Gresch, R. & Müller, W. *J. Non- Cryst. Solids*, 1979, **34**, 127.
17. Tasker, G. W., Uhlmann, D. R., Onorato, P. I. K., Alexander M. N. & Struck, C. W. *J. Phys.*, 1984, **46** (12), C8-273.
18. Matsubara, E., Sugiyama, K., Waseda, Y., Ashizuka, M. & Ishida, E. *J. Mater. Sci.*, 1990, **9**, 14.
19. Musinu, A., Piccaluga, G., Pinna, G., Vlaic, G., Narducci, D. & Pizzini, S. *J. Non-Cryst. Solids*, 1991, **136**, 198.
20. Cervinka, L., Bergerova, J. & Trojan, M. *J. Non-Cryst. Solids*, 1995, **192–193**, 121.
21. Lai, A., Musinu, A., Piccaluga, G. & Puligheddu, S. *Phys. Chem. Glasses*, 1997, **38**, 173.
22. Boiko, G. G., Andree, N. S. & Parkachev, A. V. *J. Non-Cryst. Solids*, 1998, **238**, 175.
23. Wiench, J. W., Tischendorf, B., Otaigbe, J. U. & Pruski, M. *J. Molec. Struct.*, 2002, **602–603**, 145.
24. Brow, R. K., Phifer, C. C., Turner, G. L. & Kirkpatrick, R. J. *J. Am. Ceram. Soc.*, 1991, **74** (6), 1287.
25. Dietzel, A.*Z. Elektrochem.*, 1942, **48**, 9.
26. Fayon, F., Bessada, C., Coutures, J.-P. & Massiot, D. *Inorg. Chem.*, 1999, **38**, 5212.
27. Le Saoût, G., Fayon, F., Bessada, C., Simon, P., Blin, A. & Vaills, Y. *J. Non- Cryst. Solids*, 2001, **293–295**, 657.
28. Liu, H. S., Shih, P. Y. & Chin, T. S. *Phys. Chem. Glasses*, 1996, **37** (6), 227.
29. Liu, H. S., Shih, P. Y. & Chin, T. S. *Phys. Chem. Glasses*, 1997, **38** (3), 123.
30. Liu, H. S., Chin, T. S. & Yung, S. W. *Mater. Chem. Phys.*, 1997, **50**, 1.
31. Brow R. K., Kirkpatrick, R. J. & Turner G. L. J. Am. Ceram. Soc., 1990, **73** (8), 2293.
32. Jin, Y., Jiang, D., Chen, X., Bian, B. & Huang X. *J. Non-Cryst. Solids*, 1986, **80**, 147.
33. Metwalli, E. & Brow, R. K. *J. Non-Cryst. Solids*, 2001, **289**, 113.
34. Egan, J. M., Wenslow, R. M. & Mueller, K. T. *J. Non- Cryst. Solids*, 2000, **261**, 115.
35. Montagne, L., Palavit, G., Mairesse, G., Draoui, M., Aomori, K. & Saidi Idrissi, M. *Phys. Chem. Glasses*, 1997, **38** (1), 1.
36. Massiot, D., Fayon, F., Capron, M., King, I., Le Calvé, S., Alonso, B., Durand, J.-O., Bujoli, B., Gan, Z. & Hoatson, G. *Magn. Reson. Chem.*, 2002, **40**, 70.
37. Rouse, R. B., Miller, P. J. & Risen, W. M. *J. Non-Cryst. Solids*, 1978, **28**, 193.
38. El Hezzat, M., Et-tabirou, M., Montagne, L., Palavit, G., Mazzah, A. & Dhamelincourt, P. *Phys. Chem. Glasses*, 2003, **44** (5), 345.
39. Hussin, R., Holland, D. & Dupree, R. *J. Non-Cryst. Solids*, 2002, **298**, 32.
40. Fletcher, J. P., Kirkpatrick, R. J., Howell, D. & Risbud, S. H. *J. Chem. Soc. Faraday Trans.*, 1993, **89** (17), 3297.
41. Grimmer, A.-R & Wolf, G.-U. *Eur. J. Solid State Inorg. Chem.*, 1991, **28**, 221.
42. Fayon, F., Bessada, C., Douy, A. & Massiot, D. *J. Magn. Resonance*, 1999, **137**, 116.
43. Lockyer, M. W. G., Holland, D., Howes, A. P. & Dupree, R. *Solid State Nucl. Magn. Reson.*, 1995, **5**, 23.
44. Ducel, J. F., Videau, J. J., Gonbeau D. & Pfister-Guillouzo, G. *Phys. Chem. Glasses*, 1995, **36** (6), 247.
45. Montagne, L., Palavit, G. & Mairesse, G. *Phys. Chem. Glasses*, 1996, **37** (5), 206.